Design and Simulation of Locust Beans (*Parkia Biglobosa*) Processing Plant

S. P. Ayodeji[1], R. Oboh[1], J. T. Isinkaye[1], I. A. Daniyan[*2,3,4], A. O. Adeodu[5], H. S. Phuluwa[4]

[1]Department of Industrial and Production Engineering, Federal University of Technology, Akure, Nigeria.
[2]Department of Mechatronics Engineering, Bells University of Technology, Ota, Nigeria.
[3]Centre for Artificial Intelligence, Bells University of Technology, Ota, Nigeria.
[4]Department of Industrial Engineering & Engineering Management, University of South Africa, Florida, South Africa.
[5]Department of Project Management, Bells University of Technology, Ota, Nigeria.

ABSTRACT: African locust beans (Parkia biglobosa) have a rich nutritional content and distinctive flavour, which makes it useful as a food condiment. However, its traditional processing is inefficient and labour-intensive. Hence, this study aims to design and simulate a locust bean processing plant to address challenges posed by conventional methods of locust bean production, including low production, poor packaging, seed degradation, and waste. By designing and modelling components of a processing plant using SolidWorks 2016, the study sought to modernise locust bean production techniques and create a high-quality product that can compete with other food condiments. The plant is designed to have a throughput capacity of 250 kg/hr, with the cubing blade containing 10 square cubing holes, each 20 mm × 20 mm in cross section. The finite element analysis (FEA) technique and the Von Mises stress criterion were employed to assess the structural stability of the plant's components against the functional requirements. The simulation results show that the various stresses induced in the components were below the yield strength of the selected materials, with minimal strain and displacement, and a factor of safety greater than 1. This implies that the various components will likely meet the service requirements without failing under normal operating conditions. This study presents empirical data that can help improve the design of locust bean production plants to promote high-quality production.

KEYWORDS: Food condiment, Locust beans, Modelling, Processing plant, Simulation

[Received Nov. 24, 2021; Revised May 15, 2022; Accepted May 26, 2022] Print ISSN: 0189-9546 | Online ISSN: 2437-2110

I. INTRODUCTION

The African locust beans (*Parkia biglobosa*) is produced from a perennial deciduous tree having pods that contain both sweet pulp and valuable seeds. Each of the pods has about thirty (30) seeds embedded in a sweet, powdery yellow pulp. The pods are usually harvested and processed via fermentation process into a condiment known as 'locust beans'. This condiment is known as '*Iru*' in the South-Western part of Nigeria, '*Dawadawa*' in Northern Nigeria, Niger Republic, and Ghana, '*Ogiri*' in Eastern part of Nigeria, '*Soumbala*' in Guinea, Burkina Faso, Mali and Cote d'Ivoire (Sadiku, 2010; Kourouma *et al*., 2011; Farayola *et al.,* 2012; Timothy *et al.,* 2019). Alabi *et al.* (2005) stated that locust beans seed is nutritious containing protein (40%), fat (35%), vitamins, carbohydrate with some macronutrients such as sodium, nitrogen, potassium, magnesium, soluble sugars, ascorbic acid, calcium, and phosphorus (Olajide, 2012). The cotyledon is also rich in nutrients containing less fibre and ash contents. Furthermore, the oil content is healthy for consumption since it has low acid and iodine contents (Diawara *et. al.,* 2000). The richness of locust beans in protein content implies that it could be a nutritious condiment and could serve as a supplement for protein sources such as meat, fish, etc. The results of the characterization of the locust beans (*Parkia biglobosa*) carried out by Aborisade *et al.* (2021) indicated that it consists of various major, micro, and trace nutritional elements thus making its use as a condiment beneficial to human health. Besides, it is free from toxic elements that can adversely affect the human health. Despite the rich nutritional content and distinctive flavour of locust beans and its usefulness as a food condiment, its traditional processing is inefficient and labour-intensive. Hence, the aim of this study is to design and simulate a locust beans processing plant with a view of addressing the challenges posed by traditional methods of locust bean production, such as low production, inconsistent product quality, poor packaging, seed degradation and wastage.

According to Audu *et al*. (2004), the traditional processing of locust beans seed via fermentation is usually practiced in African homes with undeveloped tools and techniques. This practice may be unhygienic, inefficient and characterised by long processing time because it relies mainly on manual labour. The traditional process which consists of de-pulping, boiling, dehulling, re-boiling, fermentation is done by covering the beans with leaves and finally, moulding the fermented beans into balls. Beaumont (2002), further emphasise that spices and additives such as salt are usually added followed by moulding the fermented beans and then sun drying to enhance the stabilization of the final condiment product. This traditional processing poses risk of contamination, inconsistent fermentation and product quality, poor packaging and limited shelf life (Yisa *et al.*, 2018). Thus, to overcome these challenges, the development of a modernized locust beans

*Corresponding author: iadaniyan@ bellsuniversity.edu. ng

doi: http://doi.org/10.63746/njtd.v22i5.3338

plant may promote food hygiene and safety, and enhance the product quality and market value, thus, making the condiment more appealing. This study is in line with the quest for a safe, standardised, and properly package food. The development of locust beans processing plant boasts of economic benefits, food security and nutritional benefits as well as social benefits (Adekaye *et al.*, 2019). For instance, the processing locust beans via a semi-autonomous system, will add market value to the condiment thereby increasing farmers' income. It will also create more employment opportunities and reduce post-harvest losses via a timely and efficient processing. This will also promote food security and improve product's shelf-life in compliance with food safety standards (Owolarafe *et al.,* 2013). Furthermore, it will contribute to the growth of small and medium scale agro industries thereby stimulating local content and economic growth. In addition, by leveraging technology, drudgery can be reduced making farmers more productive.

Research is replete with locust beans production processing and techniques. For example, Uzodinma *et al.* (2021) developed a cubing machine for processing food condiment specifically the fermented mesquite seed. The characterization of the processed fermented mesquite seed indicates that the food condiment contains maprotein (1.45–42.50%), ash (5.29–6.75%), moisture (8.50–12.29%), crude fat (2.56–18.54%), crude fibre (2.45–3.19%), and carbohydrate (18.16–25.56%). Other composition include calcium, iron, magnesium, manganese, vitamins (B1, B2, B3 and E), flavonoids (0.12–0.18%), alkaloids (0.08–0.15%), saponins (0.19–0.55%), and tannins (0.69–0.93%). This indicates that the fermented mesquite seed can be processed and cubed as a food condiment with the potential to contribute to good health and nutrition. The outcome of the study conducted by Ajayi *et al.* (2015) indicated the feasibility of using corn, cassava and potato starch extracts as binders during the processing and cubing of African locus beans (*Parkia Biglobosa*).

Gberinko *et al.* (2014) compared physicochemical properties of *Parkia Biglobosa* powdered condiments fermented with and without mixed Bacillus Species as Inocula under different drying conditions. The outcome of the investigation indicated that fast rate of fermentation at 48 h was observed for 5% inoculum *P. biglobosa* seeds compared to the fermentation without inoculum which took 72 h. Hot air oven also outperformed other drying methods such solar drying, vacuum drying and sun drying. Thus, optimum physicochemical properties of *Parkia Biglobosa* (locust beans) can be achieved with longer during storage using 5% inoculum and hot air oven drying method. Sadiku *et al*. (2010) found that the processing of locust beans without adding additives or chemical substances could produce the most nutritious beans. Atoyebi *et al.* (2022) developed computational models for the investigating the traditional and mechanised techniques processing fermented locust beans with focus is on the processing time, production ratio and rate of water. The simulation results show that the mechanized production process uses lesser quantity of water and requires shorter production cycle time, but with lower yields compared to the traditional process that requires more quantity of water and higher production cycle time but with a higher output. Okunola *et al*. (2019) developed a dehulling and washing machine for locust bean seed processing. The results of the performance evaluation indicate that the dehulling efficiency ranged from 59.7 to 68 %, while the cleaning efficiency ranged from 83.4 to 87.4 % with an average throughput capacity was 108 kg/hr. Yisa *et al.* (2018) designed a locust beans cubing machine with the capacity to cube 2 kg of fermented locust beans using a piston-connecting rod arrangement, as a conveying mechanism. Adekaye *et al.* (2019) developed a dehulling machine for locust beans processing. The machine showed throughput capacity of 264.0kg/hr, output capacity of 98.48%, recovery percentage and cleaning efficiency of 98.75% thus indicating its suitability for locust beans processing.

Other efforts made towards the development of locust beans processing machines are in the form of simple processing device (Owolarafe *et al.,* 2013) while some focused on the development of major components such as the dehuller and separator (Audu *et al.,* 2004; Adewumi 1998 & Gbabo *et al.,* 2013). The development and structural analysis of integrated plant that incorporates the various units and components for the processing of locust beans (*Parkia Biglobosa*) is the novelty for this study which has been sufficiently reported by the existing literature. This is the focal point of this study with a view to conduct structural analysis of the major components using the finite element analysis (FEA) technique in order to determine their functional capability vis-à-vis the service requirements.

The production of locust beans seed in large proportions has always been challenging. Currently, the most commonly used method of processing locust beans is the traditional method. This traditional method as identified by Akande *et al.* (2010) involve several constraints which include among others, low production, poor and obsolete processing practices, and use of rudimentary tools that result in significant seed degradation, wastage and consequential lengthy production period. Ayodeji *et al*. (2012) indicated the need to upgrade the traditional food processing and preservation methods into modern techniques to promote food and nutrition insecurity. Hence, the need to modernise locust beans production processing and techniques in order to produce high quality locust beans product that will be able to compete and replace other food seasonings. Thus, this study contributes to existing literature on the modernization of food processing techniques in terms of design analysis, modelling and simulation as well as the integration of various plant components for the processing of locust beans. It introduced a simulation-based approach into an indigenous food processing via the finite element analysis thus contributing to computational modelling of locust beans processing plants. The simulation of the structural behaviour of the plant in terms of stress distribution, strain, and deformation under the operational loading condition will assist in preventing failure, especially in critical regions or components of the processing plant such as the boiler, fermenter, dehuller, frame, dryer mixing chamber etc. thus, improving operator's safety and plant's lifespan.

Furthermore, this study provides a replicable design framework and plant's configuration that can be applied to other indigenous agro-processing plants in other regions thereby contributing to effective agro-processing plant

development. Most studies focused on the product yield, and experimentations on the conversion process. Only few studies considered the modelling and simulation of the plant's ehaviour under the required operating loads. This study conducted a multiphysics and computational modelling of the locust beans plant using the finite element analysis technique to determine the plant's structural integrity in terms of stress, strain and deformation distributions.

II. MATERIALS AND METHOD

A. System Description

The locust beans processing plant is an integrated agro-processing plant developed to process raw African locust bean seeds (*Parkia biglobosa*) into fermented locust bean condiment popularly referred to as "iru" **or "**dawadawa**"**. The plant is designed to mechanise to reduce the labour intensiveness of the traditional processing method and to improve the process hygiene, and productivity as well as product's consistency. The plant comprises of seven major units integrated into a plant. The design ensures that the units are arranged sequentially to ensure effective flow of material flow to reduce manual handling, handling time, and to reduce product's contamination.

The first unit is the raw material reception where the locust bean pods containing the seeds are received via the hopper. The pods are first boiled at the first boiling unit 100ºC for 10 hours to soften the pods and enable efficient separation of the seeds from the pods. The softened pods are thereafter moved to the dehulling unit where the seeds are separated from the pods and the seeds via are abrasion. Here, the seeds are also cleaned to remove unwanted contaminants. The chaffs and stones are removed through mechanical sieving while dirt and residual impurities are removed by washing. This unit is designed to guarantee high dehulling efficiency to ensure minimal seed breakage. Subsequently, the cleaned locust bean seeds are conveyed to the second the boiling unit designed as a thermally insulated vessel. Here, the seeds are boiled at a temperature of 100ºC for 1 hour. The design requirements ensure effective boiling to destroy harmful microorganisms while retaining the nutrients. Next to this is the fermentation unit where biochemical transformation of the cotyledons into locust bean condiment takes place for 2–4 days. It consists of fermentation trays or chambers designed to maintain suitable processing conditions such as temperature, humidity, and aeration conditions. The fermentation ensures the addition of flavour. After this, the fermented product is partially dried via mechanical heating to extend its shelf life. This unit ensures a uniform moisture removal without degrading the quality of the final product. Finally, the fermented and dried locust beans are cubed into small balls using the cubing to ensure product uniformity and to promote ease of packaging. As shown in Figure 1, the various processing units are mounted on a structural frame fabricated from mild steel. This is to support the plant to withstand static and dynamic loads, and the resulting vibration, and stresses developed during processing. To ensure that the frame withstands the various stresses developed, finite element analysis was employed to investigate the stress, strain and deformation distribution to ensure structural integrity and safety of the plant.

The design ensures improved processing efficiency and reduction in manual labour. This enhances processing hygiene and food safety.

B. Design Concept of the Locust Beans Processing Plant

The plant is designed to have a throughput capacity of 250 kg/hr with the cubing blade containing 10 square cubing holes each having a dimension of 20 mm × 20 mm in cross section. The computer aided design of the locust beans processing plant was carried out using SolidWorks software (2016 version) and analysis of each component part was done using the appropriate equations. The plant is made up of six machines, assembled, all working in a process to produce locust beans cube. These machines are boiling machine, de-husking and separation machine, fermentation machine, cubing machine, drying machine and the conveyors. The arrangement of the plant is shown in Figure 1.

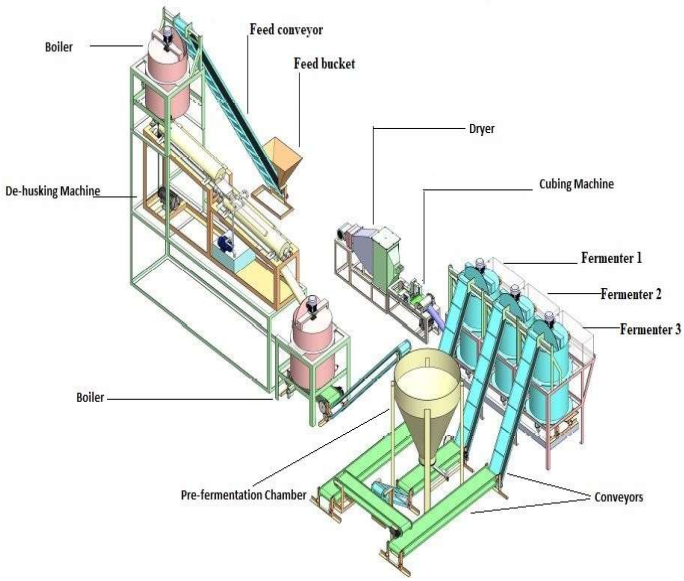

Figure 1 Computer aided design of the locust beans processing plant

The design requirements of a locust bean processing plant take into consideration factors such as hygiene of the processing unit and the non-corrosive material. Other factors considered include floor space requirement, energy consumption, availability of material, physical and mechanical properties of the material, ease of construction, maintainability and cost-effectiveness.

Simulation of the design was carried out using SolidWorks software (2016 version) to ensure functionality of the plant before production.

C. Design Analysis of Steam Boiler

The steam boiler comprises of the machine frame developed from mild steel (for support), boiler chamber, 3.3

kW electric motor (for converting electric energy into mechanical energy for driving the boiler), boiler stirrer (made of stainless steel), heating element (1000 W, 230-415V) and an actuator for controlling the valves within the system.

The energy required to heat up water to steam is estimated as 38.29 MJ using Equations (1) and (2) (Helmenstine, 2021).
The heat energy required to raise 50 kg of water at 25°C to 100°C was computed using Equation (1) as follows:

$$Q = mc\Delta T \quad (1)$$

Where Q is the heat energy (in J), m is the mass (in kg), c is the specific heat (4.184J/g·°C), and ΔT is the change in temperature (°C). Assuming that 20% of the water is converted to steam, and then the heat required was computed using Equation (2) as follows (Engineering ToolBox, 2001):

$$Q = mL \quad (2)$$

Where L is the latent heat of vaporization (2260 kJ/kg). Therefore, the heat required to heat up water to steam is (15.69 + 22.6) MJ = 38.29 MJ
The boiling chamber should be able to withstand the build in pressure in the system. At 100°C, the pressure of the steam is 1.015 bar (Rogers and Mayhew, 1995). The minimum thickness that can withstand the pressure in the steam boiler is obtained as 0.12 mm using Equation (3). 2 mm thickness was used for safety reason.

$$t = \frac{p_h D}{2\sigma_h} \quad (3)$$

Where p_h is the final and maximum pressure applied on the cylinder (Pa), D is the diameter of the cylinder (mm) and t is the thickness of the shell (mm) and σ_h is the hoop's stress (N/mm^2).

The shape of the upper of the boiler is cylindrical while the lower part is conical in shape. Thus, Equations (4), (5) and (6) (Yisa and Jiya, 2019) were used to determine the total volume that gives the volumetric capacity of the boiler.

The volume of the cylindrical part is obtained using Equation (4)

$$V_{cd} = \pi {r_{cd}}^2 h_{cd} \quad (4)$$

Where V_{cd} volume of cylinder in m^3 is, r_{cd} is radius of the cylinder and h_{cd} is height of the cylinder (mm).

The volume of the conical part is obtained by Equation (5)

$$V_{cn} = \pi {r_{cn}}^2 \frac{h_{cn}}{3} \quad (5)$$

Where V_{cn} volume of a cone (m^3) is, r_{cn} is radius of a cone and h_{cn} is height of a cone
Total volume of the steam boiler is expressed as Equation (6).

$$T_v = V_{cd} + V_{cn} \quad (6)$$

D. Design Analysis of De-husking and Separation Unit

This section comprises of a frame for support, hopper (an inlet), separation chamber, dehulling chamber, connecting shaft, pulley, electric motor and pump. The locust beans seeds are fed through the hopper and transferred to the auger in the separation chamber which separates the soft pulp and moves the material into the dehulling chamber where the seeds are washed.
For the determination of the minimum shaft diameter, the torque and moment on the shaft upon application of load were first determine. From the research done by Koya *et al.* (2011), the force required for de-hulling beans has a maximum value of 95 N at major axis. Therefore, assuming uniform de-hulling of all the locust beans with force of 95 N, the torque transmitted by the shaft is determined to be $625\ N.m$ using Equation (7) and the maximum bending moment was obtained as $47.5\ N.m$ using Equation (8). The shaft diameter of dehuller is estimated as $40\ mm$ using Equation (9) (Budynas and Nisbett, 2011, Khurmi and Gupta, 2005).

$$\tau_{dh} = n_b . F_{dh} . r_b \quad (7)$$

$$M_{dh} = F_{dh} . \frac{L_{dh}}{2} \quad (8)$$

$$d = \left\{ \frac{32.FOS}{\pi} \left[\left(\frac{k_f M_{dh}}{S_e} \right)^2 + \frac{3}{4} \left(\frac{\tau_{dh}}{S_y} \right)^2 \right]^{\frac{1}{2}} \right\}^{\frac{1}{3}} \quad (9)$$

Where n_b is the number of brushes in contact with the locust beans (120 brushes), F_{dh} is dehulling force (95 N) (Koya *et al.,* 2011), r_b is radius of the brush (mm), τ_{dh} is torque (Nmm), M_{dh} is bending moment (Nmm), L_{dh} is length of dehuller (mm), S_e is the elastic limit of the shaft material and S_y is the yield strength of the shaft material (Pa).

The de-huller brush moves such that with each rotation, the locust bean will move by 1/n of the total length of the de-hulling chamber. Where n is the total number of adjacent brushes set on the de-huller shaft. The maximum volume of locust beans that can be contained in the de-hulling chamber (V_{dh}) is given as $0.001807m^3$ using Equation (10). The volume of the total locust bean required to be de-hulled per batch is obtained as $0.18587m^3$ using Equation (11) (Okunola *et al.,* 2019). Therefore, the speed of the brush required for dehulling in 60 minutes where n is 15 adjacent brushes is estimated as $26rpm$ using Equation (12) while the speed in rad/s is given by Equation (13) (Okunola *et al.,* 2019).

$$V_{dh} = \pi \left(\frac{{d_c}^2}{4} - \frac{{d_b}^2}{4} \right) \quad (10)$$

$$V_{dh} = \pi \left(\frac{0.12^2}{4} - \frac{0.11^2}{4} \right) = 0.001807m^3$$

$$V_t = \frac{m_b}{\rho_l} \quad (11)$$

$$N_b = \frac{nV_t}{TV_{dh}} \quad (12)$$

The speed is rad/s is calculated from Equation 13 thus;

$$\omega_b = \frac{2\pi N_b}{60} \quad (13)$$

$$\omega_b = \frac{2\pi \times 26}{60} = 2.72 rad/s$$

Where V_t is the volume of the locust beans required per batch (m^3), T is time required for complete de-hulling of a batch (60 minutes), m_b is mass of the locust beans (100 kg), ρ_l is bulk density of locust beans which is 538.02 kg/m^3 (Ogunjimi *et al.,*

2002), d_c is diameter of dehulling chamber (m), d_b is diameter of the brush (m).

The power required by the shaft is the sum of power required to overcome the inertia torque and the working torque at the required speed. The inertia torque required by the shaft without load is obtained as $0.00789\,N.m$ using Equations (14) and (15). The power required for de-hulling is estimated as $1.7\,kW$ using Equation (16). Hence, the total power required to drive the de-huller and separator unit is estimated as $3.4\,kW \approx 4.5\,hp$.

$$\tau_i = I_t \frac{{\omega_b}^2}{2\pi} \quad (14)$$

$$I_t = \frac{1}{2}(m_s {r_s}^2 + m_w {r_w}^2) \quad (15)$$

$$P_T = \frac{2\pi(\tau_i + \tau_{dh})N_b}{60} \quad (16)$$

Where τ_i is inertia torque $(N.m)$, I_t is mass moment of inertia (kg.m^2), m_s is the mass of the shaft (m), m_w is the mass of the wood (m), r_s is the radius of the shaft (m), r_w is the radius of the wood (m) and ω_b is speed (rad/s).

E. Design Analysis of the Fermentation Unit

This unit comprises of the frame, fermentation chamber, electric motor, actuator, stirrer shaft, housing for inoculant. The fermentation process usually takes time t_f for adequate fermentation. During this process, the temperature needs to be conditioned and the bacteria (h) need to be added to the sample. Also, due to sticky nature of the fermented condiments, there is a need for a stirrer to be incorporated so as to free the sticky condiment when discharging.

The force required to turn the condiment was determined to be 129.3 N using Equation (17), while the torque required to turn the condiment was determined to be 568.93 N.m using Equation (18). Since no bending moment is applied, the diameter was estimated to be 50 mm using Equation (19) (Khurmi and Gupta, 2005).

$$F_b = m_f \frac{\rho\pi\ {f}^2 w_s}{4} g \quad (17)$$

$$\tau_b = n_s F_b \times l_{st} \quad (18)$$

$$d = \left\{ \frac{32n}{\pi} \left[\frac{3}{4} \left(\frac{\tau_T}{S_y} \right)^2 \right]^{\frac{1}{2}} \right\}^{\frac{1}{3}} \quad (19)$$

Where F_b force required to turn locust beans (N), m_f is the material factor equal to 1.7, R_f is the radius of the fermenter (m), ρ_{lb} is the bulk density of the locust beans which is 538.02 kg/m^3 (Ogunjimi *et al.,* 2002), w_{st} is the width of the stirrer arm (m), n_s is the number of stirrer arms in the stirrer shaft, l_{st} is the length of the stirrer arm (m), n is the safety factor, S_e is the elastic limit of the shaft material and S_y is the yield strength of the shaft material (Pa).

The speed for turning should be one revolution in two second i.e. 30 rpm. Using Equation (20) (Okunola *et al.,* 2019), the angular speed required is π, while the inertia torque required to turn the stirrer mechanism from Equation (21) is given as $26.42\,N.m$. The total force required from the prime mover is calculated to be $595.35\,N.m$ using Equation (22). Therefore, the power from electric motor required to turn the stirrer mechanism is estimated as $1870\ \text{W} \approx 2.5hp$ using Equation (23).

$$\omega_s = \frac{2\pi N}{60} = \pi \quad (20)$$

$$\tau_i = \left(\pi \frac{{r_s}^4 L_s}{2} + n_s t_{st} w_{st} {l_{st}}^3 \right) \rho_s \frac{{\omega_s}^2}{2\pi} \quad (21)$$

$$\tau_T = \tau_i + \tau_b \quad (22)$$

$$P_s = \tau_T \times \omega_s \quad (23)$$

Where r_s is the radius of the stirrer shaft (m), L_s is the length of the stirrer shaft (m), t_{st} is the thickness of the stirrer arm (m), ρ_s is the density of the stirrer material (kg/m^3) ω_s is the speed of the stirrer (rad/s).

F. Design Analysis of Cubing Unit

The cubing unit comprises of the frame, cubing cutter, electric motor, linear actuator, pulley, blade carrier, auger shaft, conveyor belt, and rollers.

The auger shaft serves the purpose of compressing the particles and at same time conveying the compressed particles through the die to the cubing chamber. The important parameter for the design of the auger shaft is its required pitch expressed by Equation (24).

$$p = \frac{4v d_i L_{as}}{\pi \omega_{as} ({d_o}^2 - {d_i}^2)} \quad (24)$$

Where v is velocity of flow of the condiment (m/s), d_i is internal diameter of auger shaft (m) L_{as} is the length of the auger shaft (m), and ω_{as} is the speed of the auger shaft (rad/s).

The cubing compartment consists of a vertically positioned actuator to which the chassis of the cubing blades is attached. The actuator operates vertically in a regular up-and-down motion with the attached blades cutting the compacted locust beans at regular intervals and at a preset dimension. The cubing blade comprises wire mesh having10 square cubing holes each having a dimension of 20 mm × 20 mm in cross section.

The size of each of the holes in the mesh was determined using Equation (25) (Khurmi and Gupta, 2005, Uzodinma *et al.,* 2021).

$$S = 6a^2 \quad (25)$$

Where a is length of sides (20 mm) and S is size of hole, meshing the cubing compartment (mm^2)

Therefore, the size of each cubed condiment produced is 0.0024 m^2.

G. Design Analysis of Dryer

The drying system works by vaporizing water from the condiment. To achieve this, the heat that must be supplied for drying to occur has to be equivalent to the heat required for vaporization of water.

The mass of water to be expelled from a batch of 100kg/hr is $(20\% \times 100)$ is $20kg$.

Therefore, from Equation (26), the energy required for heating is determined to be 45200 kJ. The electrical power required for obtaining such energy with minimum efficiency of 80% is estimated to be 15.7 kW using Equation (27).

$$H = m_w L_h \quad (26)$$

$$P_d = \frac{H}{\eta t_{ds}} \quad (27)$$

Where L_h is the latent heat of vaporization of water (2260 kJ/kg) (Engineering ToolBox, 2001), m_w is the mass of water present in the material (kg), η is the heating efficiency of the system considering heat transfer and t_{ds} is the allotted time required for drying (s).

H. Design Analysis of Conveyor

In the analysis of the conveyor, the important parameters required are the torque required to carry the given capacity, and the speed required to deliver under the specified time.

To determine the power, the torque required by the conveying system was first determined using Equation (28), while the speed of the conveyor required is given by Equation (29). Therefore, the power required by the conveyor is determined using Equation (30).

$$\tau_{c1} = \frac{C}{3600} \times g \times t_{ct} \times L_{cb} + \rho_R \pi \frac{{D_{cb}}^3}{2} t_R l_{cb} \quad (28)$$

$$N_{cb} = \frac{60 L_{cb}}{\pi t_{ct} D_{cb}} \quad (29)$$

$$P_{c1} = \tau_{c1} \times \frac{2\pi N_{c1}}{60} \quad (30)$$

where C is capacity of the system in kg/hr, t_{ct} is the time required to convey the locust bean (s), L_{cb} is the length of the conveyor (m), D_{cb} is the diameter of the conveyor roller (m), ρ_R is the density of material of the conveyor's roller (kg/m^3), l_{cb} is the length of the conveyor's roller (m) and t_R is the thickness of the roller (m).

I. Simulation Study of the Processing Plant

The workability, functionality and structural stability of the processing plant's design were evaluated by simulating its designed model using SolidWorks (CAD software, 2016 version). The finite element analysis (FEA) is a numerical method used for investigating of the behaviours of a compo*nen*t or assembly under specified conditions (Daniyan *et al.,* 2024; Fameso *et al.,* 2020a; Muvunzi *et al.,* 2022). The FEA to determine the ability of the designed plant to withstand the applied load under normal working condition and validate product quality performance and safety throughout the design in static and dynamic environment (Oyesola *et al.,* 2022; Fameso & Desai 2020b). The first step in implementing the FEA technique in the SolidWorks environment is the determination of the study type. For this study, the static (or stress) study was selected. The static study calculates the magnitude of the stresses induced in the component part and their corresponding strain, displacements, reaction forces, and factor of safety. The failure analysis was carried out using the Von Mises failure criterion. Next is the assignment of the materials for each of the components simulated. These include: the boiling unit, de-husking unit, fermentation unit, cubing and drying unit. The materials used for the components were selected from the database or library having the mechanical properties of the selected materials required to solve the analysis. In the third consists of the free body diagram which indicates the behaviours of the components under the required conditions. The components were subjected to load analysis through simulation runs. During simulation, load of about 1000 N was uniformly distributed on the component parts. This is followed with the discretization of the models into finite elements using solid meshes whose size ranges from 2.0 to 2.6 for the various components. The simulations are run and the areas where induced stress, static displacement and static strain were significant are noted. The results obtained from the evaluation were then tabulated. The mesh size plays an important role in obtaining accurate finite element results at an optimum computing time being a major determinant of the number elements involved.

Figure 2 presents the computational time against the mesh using a mesh interval of 0.2 mm for the boiling unit. The mesh size of 2.4 mm which gave the least computational time of 129 s was employed for meshing the models into finite elements. The same process was repeated for other components such as the de-husking unit, fermentation unit, cubing and drying unit and the meshing sizes obtained rages from a minimum value of 2.0 mm to a maximum value of 2.6 mm.

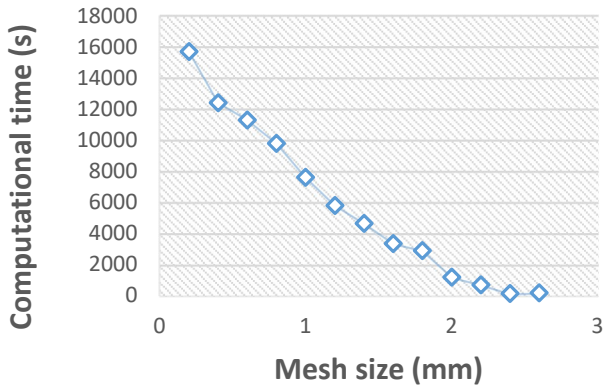

Figure 2 Mesh size and computational time for the boiling unit

Table 1 presents the details of the materials for some parts of the locust beans processing plant.

Table 1: The materials selected for the locust beans processing plant

S/N	Machine component	Selected Materials	Reasons for Selecting the Material
1	Machine frame	Mild steel	Suitable, readily available and has excellent strength
2	Receiving hopper	Stainless steel	Suitable and readily available
3	Boiler Chamber	Stainless steel	Suitable for food processing and corrosion resistant
4	Boiler stirrer	Mild steel	Suitable, cost effective and readily available
5	Dehuller brush	Rubber	Suitable for food processing and corrosion resistant
6	Dehulling Chamber	Stainless steel	Suitable for food processing and corrosion resistant

7	Separation chamber	Stainless steel	It is suitable and readily available
8	Water pump	Not Applicable	It is suitable and readily available
9	Connecting shaft	Mild steel	Cost-effective and readily available
10	Pulley	Mild steel	Cost-effective and readily available
11	Fermentation inner chamber	Stainless steel	Suitable for food processing and corrosion resistant
12	Fermentation outer chamber	Mild steel	Cost-effective, readily available and has excellent strength
13	Fermenter lagging material	Saw dust	Suitable, cost-effective and readily available
14	Stirrer shaft	Mild steel	Suitable and readily available
15	Housing for inoculant	Plastic	Suitable, readily available, cost-effective, non-reactive and transparent
16	Grinding drum	Mild steel	Suitable, cost-effective and readily available
17	Grating disc	Mild steel	Suitable, cost effective, good strength, and readily available
18	Delivery chute	Mild steel	Suitable, cost-effective and readily available
19	Cubing cutter	Stainless steel	Suitable for food processing, and corrosion resistant
20	Blade carrier	Mild steel	Suitable, It is cheap, readily available
21	Auger shaft	Stainless steel	Suitable for food processing, and corrosion resistant
22	Rollers	Mild steel	Suitable, readily available, cost-effective and has excellent strength
23	Drying chamber	Mild steel	Suitable, cost-effective and readily available
24	Insulator	Hardboard	low thermal conductivity, cost-effective and readily available
25	Dryer Tray	Aluminium	Good thermal conductivity and cost-effective
26	Blower		Suitable and cost-effective
27	Conveyor belt	Rubber	Suitable, readily available and cost-effective
28	Heating element		Suitable, readily available and cost-effective
29	Electric motors		Suitable, readily available and cost-effective
30	Linear Actuators	12 V 50 mm 9 mm/s Load: 30 N	Suitable, readily available and cost-effective

III. RESULTS AND DISCUSSION

A. Design Evaluation of Boiler Unit

The results of the boiler chamber's stress distribution is presented in Figure 3 while Table 2 presents its static displacement, strain energy and factor of safety (FOS). As displayed in Figure 3, the red portion in the legend shows areas where the stresses are maximal, while the portion in the blue colour shows where stresses are minimal. The result shows that the highest stress is 1.162 x 10^7 N/m^2 which is lower than the yield stress of stainless steel (2.40 x 10^8 N/m^2), used for the design. Fameso *et al.* (2022) indicate that when the stress induced in a material is lower than the yield strength of the material, there is a high feasibility that material is suitable for the intended application. This implies that the boiler chamber is unlikely to yield to failure under the loading requirements using the selected material (stainless steel).

Furthermore, the minimum factor of safety as shown in Table 2 is 19 (FOS > 1), 1.which show that the design is safe.

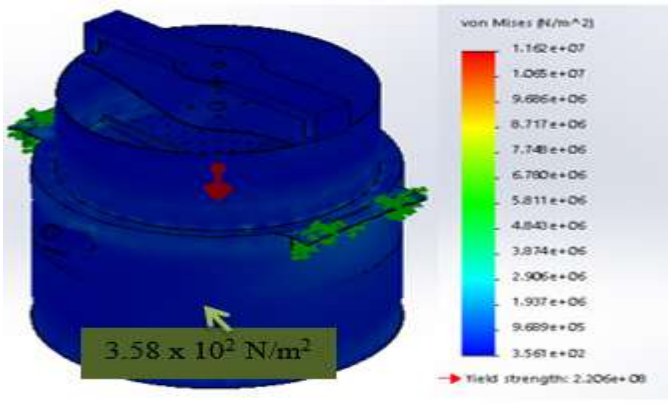

Figure 3 Stress distribution on the boiler chamber

Table 2 Simulation results of the boiler chamber

Stress distribution(N/m^2)	**Static displacement (mm)**	**Static strain**	**FOS**
1.162 x 10^7	3.240 x 10^{-2}	4.246 x 10^{-5}	6.195 x 10^5
1.065 x 10^7	2.970 x 10^{-2}	3.892 x 10^{-5}	5.679 x 10^5
9.686 x 10^6	2.700 x 10^{-2}	3.538 x 10^{-5}	5.163 x 10^5
8.717 x 10^6	2.430 x 10^{-2}	3.184 x 10^{-5}	4.646 x 10^5
7.748 x 10^6	2.160 x 10^{-2}	2.831 x 10^{-5}	4.130 x 10^5
6.780 x 10^6	1.890 x 10^{-2}	2.477 x 10^{-5}	3.614 x 10^5
5.811 x 10^6	1.620 x 10^{-2}	2.123 x 10^{-5}	3.098 x 10^5
4.843 x 10^6	1.350 x 10^{-2}	1.769 x 10^{-5}	2.581 x 10^5
3.874 x 10^6	1.080 x 10^{-2}	1.415 x 10^{-5}	2.065 x 10^5
2.906 x 10^6	8.099 x 10^{-3}	1.062 x 10^{-5}	1.549 x 10^5
1.937 x 10^6	5.400 x 10^{-3}	7.078 x 10^{-6}	1.033 x 10^5
9.689 x 10^5	2.700 x 10^{-3}	3.539 x 10^{-6}	5.164 x 10^4
3.561 x 10^5	1.000 x 10^{-30}	1.412 x 10^{-9}	19

Figure 4 presents the stress distribution of the boiler frame while Table 3 presents its static displacement, strain energy and factor of safety (FOS). As shown in Figure 4, the induced stress was observed to be at a maximum value of 2.045 x 10^7 N/m^2 at the top part of the frame structure. This causes static displacement at maximum value of 0.779 mm at the center of the structure while static strain was observed to be at the maximum level of 3.889 x 10^{-5} at the upper parts near the weld. However, it is observed that the induced stress was below the yield strength (2.20594 x 10^8 N/m^2) of plain carbon steel

selected for the frame structure with the minimum FOS being 11. This implies that using the selected material, the boiler frame possesses sufficient strength and rigidity to withstand the loading requirements without yielding to failure.

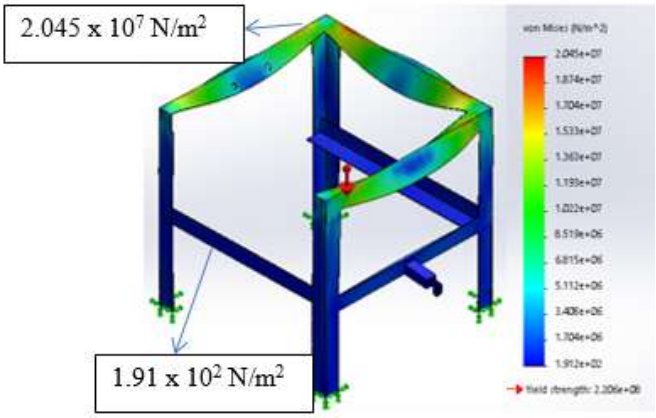

Figure 4 Stress distribution on the boiler frame

Table 3 Simulation results of the boiler frame

Stress distributions (N/m^2)	Static displacement (mm)	Static strain	FOS
2.045×10^7	7.796×10^{-1}	3.889×10^{-5}	1.154×10^6
1.874×10^7	7.148×10^{-1}	3.565×10^{-5}	1.058×10^6
1.704×10^7	6.498×10^{-1}	3.241×10^{-5}	9.614×10^5
1.533×10^7	5.849×10^{-1}	2.971×10^{-5}	8.653×10^5
1.363×10^7	5.199×10^{-1}	2.593×10^{-5}	7.691×10^5
1.193×10^7	4.549×10^{-1}	2.269×10^{-5}	6.730×10^5
1.022×10^7	3.899×10^{-1}	1.945×10^{-5}	5.768×10^5
8.519×10^6	3.249×10^{-1}	1.621×10^{-5}	4.807×10^5
6.815×10^6	2.599×10^{-1}	1.296×10^{-5}	3.846×10^5
5.112×10^6	1.950×10^{-1}	9.723×10^{-6}	2.884×10^5
3.408×10^6	1.300×10^{-1}	6.483×10^{-6}	1.923×10^5
1.704×10^6	6.498×10^{-1}	3.242×10^{-6}	9.615×10^4
1.912×10^2	1.000×10^{-30}	6.725×10^{-10}	1.079×10^1

B. Design Evaluation of De-husking and Separation Unit

The stress distribution of the de-husking chamber is shown in Figure 5. The maximum induced stress (4.954×10^6 N/m^2), static displacement (0.0278 mm) and strain (1.598×10^{-5}) were located at the two side of the chamber close to the centre. This is caused by the concentration of weight of the beans and other accessories on the two points. The maximum induced stress is still acceptably below the yield strength (2.20594×10^8 N/m^2) of the plain carbon steel selected for the development of the de-husking chamber with the minimum FOS being 45 as shown in Table 4. This implies that the de-husking chamber will unlikely yield to failure under the loading requirement using the selected material.

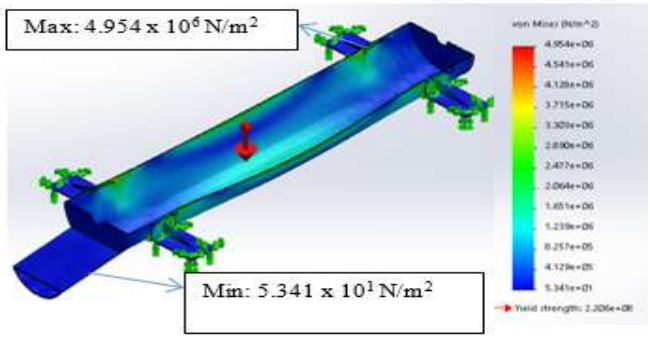

Figure 5 Stress distribution on the de-husker

Table 4 Simulation results of the de-husking chamber

Stress distributions (N/m^2)	Static displacement (mm)	Static strain	FOS
4.954×10^6	2.785×10^{-2}	1.598×10^{-5}	4.130×10^6
4.541×10^6	2.553×10^{-2}	1.465×10^{-5}	3.786×10^6
4.128×10^6	2.321×10^{-2}	1.332×10^{-5}	3.442×10^6
3.715×10^6	2.089×10^{-2}	1.198×10^{-5}	3.098×10^6
3.303×10^6	1.857×10^{-2}	1.065×10^{-5}	2.753×10^6
2.890×10^6	1.625×10^{-2}	9.322×10^{-6}	2.409×10^6
2.477×10^6	1.393×10^{-2}	7.990×10^{-6}	2.065×10^6
2.064×10^6	1.161×10^{-2}	6.658×10^{-6}	1.721×10^6
1.651×10^6	9.284×10^{-3}	5.327×10^{-6}	1.377×10^6
1.239×10^6	6.963×10^{-3}	3.995×10^{-6}	1.033×10^6
8.257×10^5	4.642×10^{-3}	2.663×10^{-6}	6.884×10^5
4.129×10^5	2.321×10^{-3}	1.332×10^{-6}	3.442×10^5
5.341×10^1	1.000×10^{-30}	1.886×10^{-10}	4.453×10^1

Figure 6 presents the stress distribution on the separating chamber while Table 5 presents its static displacement, strain energy and factor of safety (FOS). As displayed in Figure 6, the induced stress (1.132e+06 N/m^2), and static strain (6.364e-06) obtained were observed to be located at the areas around the weld of the part affixed to the frame where, the far end of the output cylinder will have displacement of less than 0.015

mm. Since the induced stress is lower than the material's yield strength and the minimum factor of safety as shown in Table 5 is 114 (FOS > 1), it implies that the separating chamber is unlikely to yield to failure under the loading requirements using the selected material.

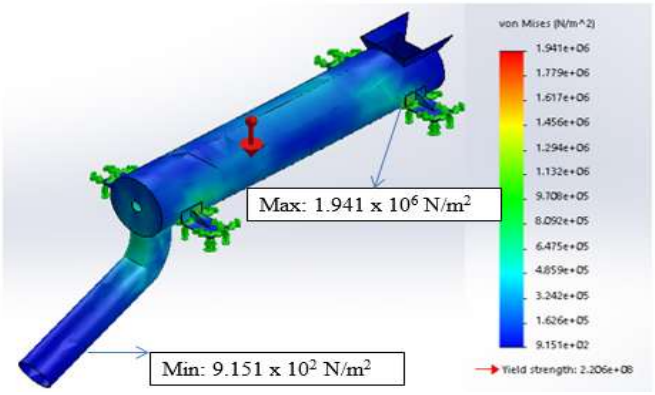

Figure 6 Stress distribution on the separation chamber

Table 5 Simulation results of the separation chamber

Stress distribution (N/m^2)	Static displacement (mm)	Static strain	FOS
1.941×10^6	1.463×10^{-2}	6.364×10^{-6}	2.411×10^5
1.779×10^6	1.341×10^{-2}	5.834×10^{-6}	2.210×10^5
1.617×10^6	1.219×10^{-2}	5.304×10^{-6}	2.009×10^5
1.456×10^6	1.097×10^{-2}	4.774×10^{-6}	1.808×10^5
1.294×10^6	9.752×10^{-3}	4.244×10^{-6}	1.607×10^5
1.132×10^6	8.533×10^{-3}	3.714×10^{-6}	1.407×10^5
9.708×10^5	7.314×10^{-3}	3.184×10^{-6}	1.206×10^5
8.092×10^5	6.095×10^{-3}	2.654×10^{-6}	1.005×10^5
6.475×10^5	4.876×10^{-3}	2.124×10^{-6}	8.043×10^4
4.859×10^5	3.657×10^{-3}	1.594×10^{-6}	6.035×10^4
3.242×10^5	2.438×10^{-3}	1.064×10^{-6}	4.027×10^4
1.626×10^5	1.219×10^{-3}	5.336×10^{-7}	2.019×10^4
9.151×10^2	1.000×10^{-30}	3.559×10^{-9}	1.137×10^2

C. Design Evaluation of Fermentation Unit

The results of the fermentation's chamber's stress distribution are presented in Figure 7 while Table 6 presents its static displacement, strain energy and factor of safety (FOS). As displayed in Figure 7, the maximum induced stress (9.092 x 10^6 N/m2) and strain energy (2.498e-05) obtained is located in the part around the chamber where flange fixed to the frame is welded to the chamber. The flange exhibits maximum displacement of 0.03 mm. Since the induced stress is lower than the material's yield strength and the minimum factor of safety as shown in Table 6 is 5 (FOS > 1), it implies that the fermentation chamber is unlikely to yield to failure under the loading requirements using the selected material.

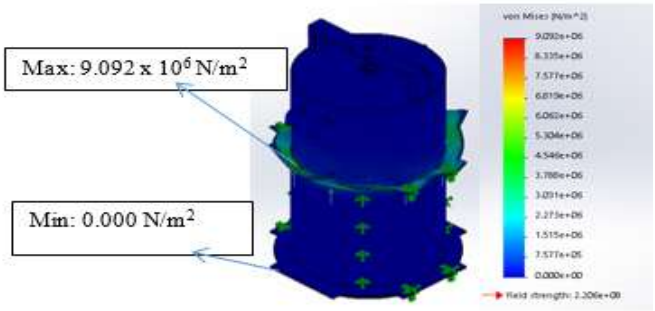

Figure 7 Stress distribution on the fermenter

Table 6 Simulation results of the fermentation chamber

Stress distributions (N/m^2)	Static displacement (mm)	Static strain	FOS
9.092×10^6	2.967×10^{-2}	2.498×10^{-5}	5.005
8.335×10^6	2.720×10^{-2}	2.290×10^{-5}	5.005
7.577×10^6	2.473×10^{-2}	2.081×10^{-5}	5.004
6.819×10^6	2.225×10^{-2}	1.873×10^{-5}	5.004
6.062×10^6	1.978×10^{-2}	1.665×10^{-5}	5.003
5.304×10^6	1.731×10^{-2}	1.457×10^{-5}	5.003
4.546×10^6	1.484×10^{-2}	1.249×10^{-5}	5.003
3.788×10^6	1.236×10^{-2}	1.041×10^{-5}	5.002
3.031×10^6	9.890×10^{-3}	8.325×10^{-6}	5.002
2.273×10^6	7.418×10^{-3}	6.244×10^{-6}	5.001
1.515×10^6	4.945×10^{-3}	4.163×10^{-6}	5.001
7.577×10^5	2.473×10^{-3}	2.081×10^{-6}	5.000
0.000	1.000×10^{-30}	0.000	5.000

Figure 8 presents the stress distribution of the fermenter frame while Table 7 presents its static displacement, strain energy and factor of safety (FOS). As displayed in Figure 8, the induced stress was observed to be at the maximum of 4.487 x

10^7 N/m^2 at the top part of the frame structure. This causes static displacement at maximum level of 0.966 mm and static strain (1.075 x 10^{-4}) at the top part of the structure. The minimum FOS is observed to be 4.9 and this is seen at the upper parts near the weld. Since the induced stress is lower than the material's yield strength and the minimum factor of safety as shown in Table 7 is 4.9 (FOS > 1), it implies that the fermenter frame is unlikely to yield to failure under the loading requirements using the selected material.

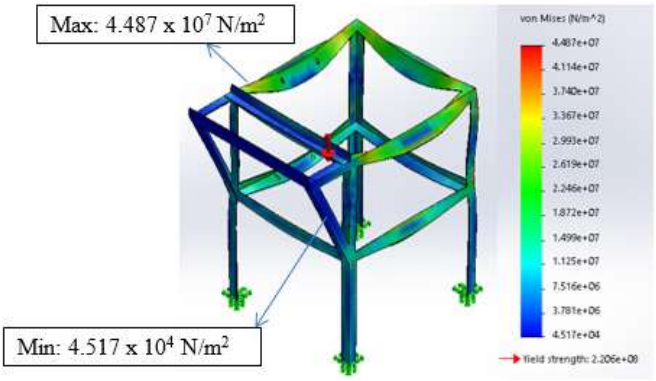

Figure 8 Stress distribution on the fermenter frame

Table 7 Simulation results of the fermentation chamber

Stress distributions (N/m^2)	**Static displacement (mm)**	**Static strain**	**FOS**
4.487 x 10^7	9.657 x 10^{-1}	1.075 x 10^{-4}	10
4.114 x 10^7	8.85e2 x 10^{-1}	9.859 x 10^{-5}	9.6
3.740 x 10^7	8.047 x 10^{-1}	8.964 x 10^{-5}	9.2
3.367 x 10^7	7.243 x 10^{-1}	8.069 x 10^{-5}	8.7
2.993 x 10^7	6.438 x 10^{-1}	7.174 x 10^{-5}	8.3
2.619 x 10^7	5.633 x 10^{-1}	6.279 x 10^{-5}	7.9
2.246 x 10^7	4.828 x 10^{-1}	5.383 x 10^{-5}	7.5
1.872 x 10^7	4.024 x 10^{-1}	4.488 x 10^{-5}	7.0
1.499 x 10^7	3.219 x 10^{-1}	3.593 x 10^{-5}	6.6
1.125 x 10^7	2.414 x 10^{-1}	2.698 x 10^{-5}	6.2
7.516 x 10^6	1.609 x 10^{-1}	1.803 x 10^{-5}	5.8
3.781 x 10^6	8.047 x 10^{-2}	9.079 x 10^{-6}	5.3
4.517 x 10^4	1.000 x 10^{-30}	1.284 x 10^{-7}	4.9

D. Design Evaluation of Cubing Unit

Figure 9 presents the stress distribution of the auger shaft while Table 8 presents its static displacement, strain energy and factor of safety (FOS). As displayed in Figure 9, it can be seen that 6.517 x10^7 N/m^2 is maximum stress induced in the auger shaft due to loads and boundary conditions. The static displacement (0.1 mm) was observed to be located at the center part along the shaft blade. The induced stress was below the yield strength (2.20594e+08 N/m^2) of the mild steel selected for the shaft with FOS of 3.4. Since the induced stress is lower than the material's yield strength and the minimum factor of safety as shown in Table 8 is 3.4 (FOS > 1), it implies that the auger shaft is unlikely to yield to failure under the loading requirements using the selected material.

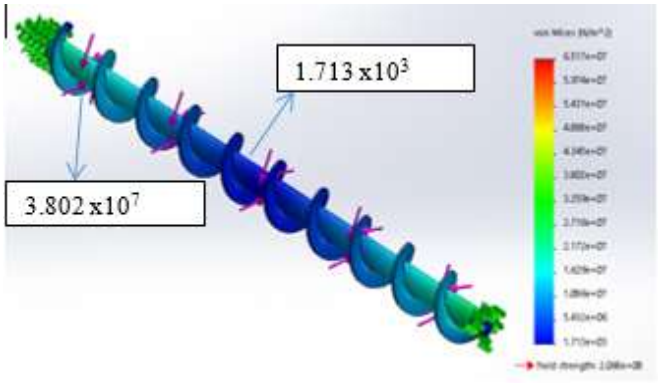

Figure 9: Stress distribution on the auger shaft

Table 8: Simulation results of the auger shaft

Stress distributions (N/m^2)	Static displacement (mm)	Static strain	FOS
6.517 x 10^7	1.080 x 10^{-1}	3.143 x 10^{-4}	3.4
5.974 x 10^7	9.903 x 10^{-2}	2.882 x 10^{-4}	3.6
5.431 x 10^7	9.003 x 10^{-2}	2.620 x 10^{-4}	4.1
4.888 x 10^7	8.103 x 10^{-2}	2.358 x 10^{-4}	4.5
4.345 x 10^7	7.203 x 10^{-2}	2.096 x 10^{-4}	5.1
3.802 x 10^7	6.302 x 10^{-2}	1.834 x 10^{-4}	5.8
3.259 x 10^7	5.402 x 10^{-2}	1.572 x 10^{-4}	6.8
2.716 x 10^7	4.502 x 10^{-2}	1.310 x 10^{-4}	8.1
2.172 x 10^7	3.601 x 10^{-2}	1.048 x 10^{-4}	10.2
1.629 x 10^7	2.701 x 10^{-2}	7.859 x 10^{-5}	13.5
1.086 x 10^7	1.802 x 10^{-2}	5.240 x 10^{-5}	20.3
5.432 x 10^6	9.003 x 10^{-3}	2.620 x 10^{-4}	40.6
1.713 x 10^3	1.000 x 10^{-30}	8.295 x 10^{-9}	1.3 x 10^5

E. Design Evaluation of Drying Unit

The results of the dryer frame stress distribution is presented in Figure 10 while Table 9 presents its static displacement, strain

energy and factor of safety (FOS). From Figure 10, it can be seen that 1.267 x 10^7 N/m^2 was maximum stress induced in the dryer frame due to loads and boundary conditions. The static displacement (0.07 mm) was observed to be located at the upper part of the frame structure. The induce stress was below the yield strength (**2.20594e+08** N/m^2) of the mild steel selected for the shaft with an FOS of 17. Since the induced stress is lower than the material's yield strength and the minimum factor of safety as shown in Table 9 is 17 (FOS > 1), it implies that the dryer frame is unlikely to yield to failure under the loading requirements using the selected material.

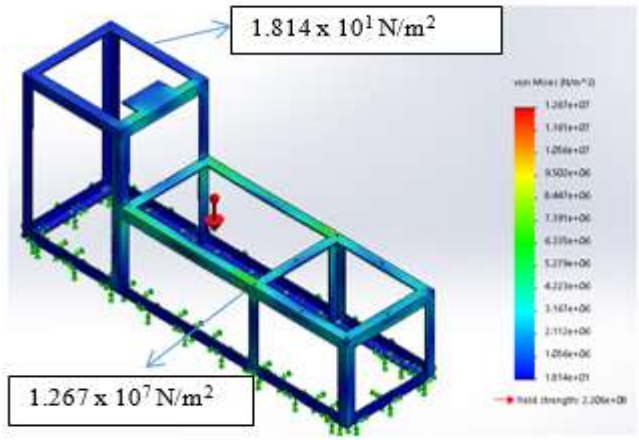

Figure 10: Stress distribution on the dryer frame

Table 9: Simulation results of the cutter frame

Stress distribution (N/m^2)	Static displacement (mm)	Static strain	FOS
1.267 x 10^7	7.234 x 10^{-2}	3.802 x 10^{-5}	1.741 x 10^1
1.161 x 10^7	6.631 x 10^{-2}	3.485 x 10^{-5}	1.014 x 10^6
1.056 x 10^7	6.028 x 10^{-2}	3.169 x 10^{-5}	2.027 x 10^6
9.502 x 10^6	5.425 x 10^{-2}	2.852 x 10^{-5}	3.041 x 10^6
8.447 x 10^6	4.823 x 10^{-2}	2.535 x 10^{-5}	4.054 x 10^6
7.391 x 10^6	4.220 x 10^{-2}	2.218 x 10^{-5}	5.068 x 10^6
6.335 x 10^6	3.617 x 10^{-2}	1.901 x 10^{-5}	6.081 x 10^6
5.279 x 10^6	3.014 x 10^{-2}	1.584 x 10^{-5}	7.095 x 10^6
4.223 x 10^6	2.411 x 10^{-2}	1.267 x 10^{-5}	8.108 x 10^6
3.167 x 10^6	1.808 x 10^{-2}	9.506 x 10^{-6}	9.122 x 10^6
2.112 x 10^6	1.206 x 10^{-2}	6.337 x 10^{-6}	1.014 x 10^7
1.056 x 10^6	6.028 x 10^{-3}	3.169 x 10^{-6}	1.115 x 10^7
1.814 x 10^1	1.000 x 10^{-30}	1.276 x 10^{-10}	1.216 x 10^7

The components' responses to external forces and loading conditions show the effects of mechanical loading. However, the Von Mises stress distributions of the components do not pose any threats to the stability or performance of the components under the required operating conditions. It is evident that the stresses developed in the components do not result in significant buckling, distortion or deformation as the various material's yield strength were not exceeded. The induced stresses and displacements in the components may be due to torsional moments, load concentration coupled with thermal, pressure and centrifugal loading or any combination of these (Oyesola *et al.,* 2022). Furthermore, the different loads aggregation may cause slight displacement with the deformation attributable to the loading regimes (centrifugal, thermal, or pressure) imposed on the components. It can be inferred that the higher the magnitudes of imposed loads beyond the ones considered for the simulation, the more the components' integrity are pushed beyond the safe limits. The strain profiles of the components are predominantly elastic in nature with zero plastic strains. Thus, the results obtained show that the selected materials will meet the functional requirements having shown feasibility to withstand applied forces and loads without yielding to failing since the resultant internal stresses, fall within allowable ranges. This shows good structural stability of the components without any significant deformation or failure.

F. Design Evaluation of De-husking Brush

Figure 11 illustrates the static stress and displacement of the de-husking brush. From Figure 11a, the maximum induced stress (7.281e+05 N/m^2) is observed to be acceptably below the yield strength of the selected material with minimum factor of safety of 3e+02 as shown in Table 10. However, the maximum static displacement (6.091e-04 mm) is evenly distributed at the center of the brush as seen in Figure 11b which is attributed to the concentration of the weight of the beans in that part of the structure and the length of the brush.

Also, in a dynamic environment as presented in Figure 12 (a & b), at a model frequency of 17.77 Hz, the maximum stress is 4.716e+02 N/m^2 with a maximum vibration amplitude value of 1.716e-06 mm though negligible, is located at the center part of the brush.

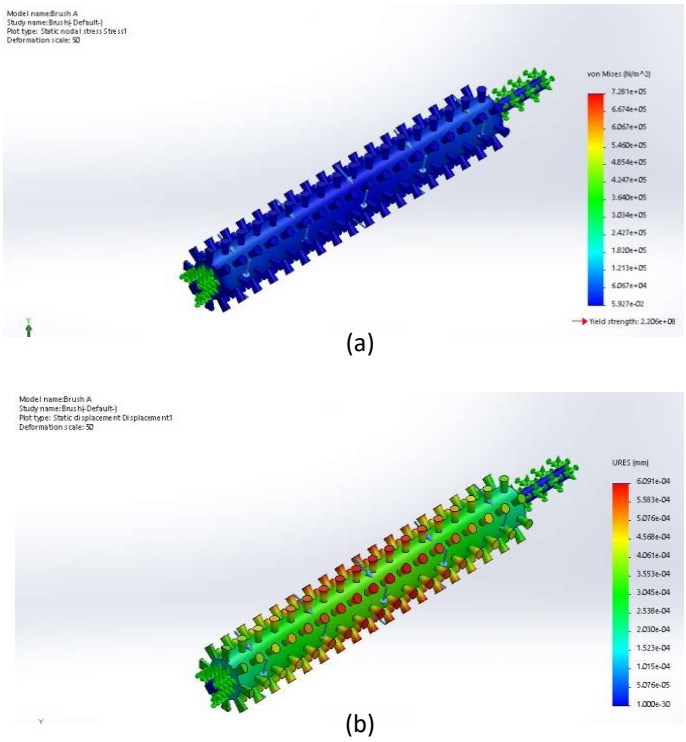

Figure 11: Static (a) stress distributions and (b) displacements of de-husking brush

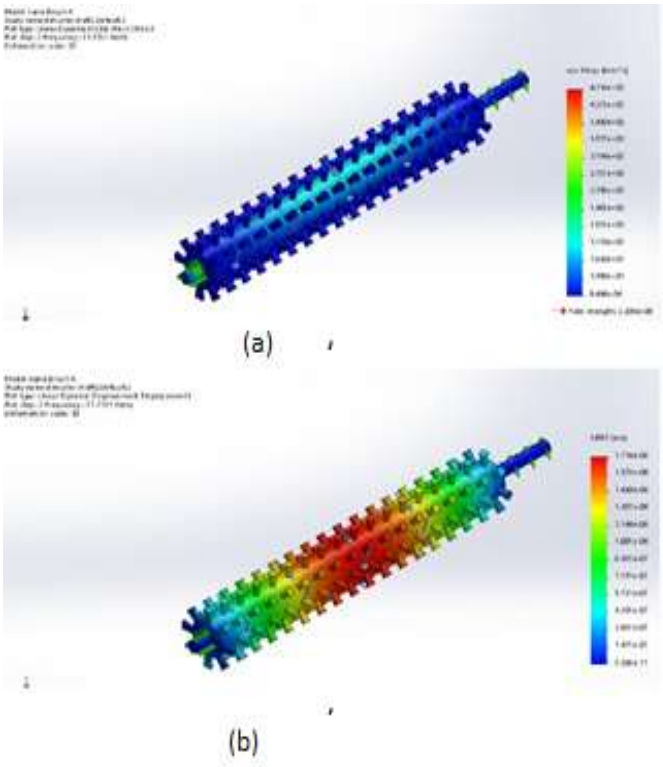

Figure 12: Dynamic (a) stress distributions and (b) displacements of de-husking brush

Table 10: FOS of key components of locust beans processing plant

De-husking brush	Fermenter stirrer	Auger shaft
3.030×10^{2}	3.36×10^{1}	3.4
3.102×10^{8}	3.67×10^{1}	3.6
6.203×10^{8}	4.04×10^{1}	4.1
9.305×10^{8}	4.48×10^{1}	4.5
1.241×10^{9}	5.04×10^{1}	5.1
1.551×10^{9}	5.76×10^{1}	5.8
1.861×10^{9}	6.73×10^{1}	6.8
2.171×10^{9}	8.07×10^{1}	8.1
2.481×10^{9}	1.01×10^{2}	10.2
2.791×10^{9}	1.35×10^{2}	13.5
3.102×10^{9}	2.02×10^{2}	20.3
3.412×10^{9}	4.04×10^{2}	40.6
3.722×10^{9}	5.63×10^{3}	1.3×10^{5}

G. Design Evaluation of Fermentation Stirrer

Results of the stirrer's stress and static displacement are presented in Figure 13 (a & b). The result shows that the maximum induced stress (6.559e+06 N/m^2) obtained is located in the part around the wed between the flange and the shaft. This is attributed to the turning effect of the shaft as it pulls the locust beans. Also, the far end of the flange exhibit maximum displacement of 0.36 mm. However, the induced stress was observed to be acceptably below the yield strength (2.206e+08 N/m^2) of the selected material while the displacement is very small as such, it is negligible.

From the dynamic analysis illustrated in Figure 14 (a & b), at a model frequency of 6.1 Hz, the maximum dynamic stress is 3.364e+06 N/m^2 which is far below the yield strength of the selected material. Also, from the vibration amplitude shown in Figure 5b, the maximum vibration amplitude is very low at a value of 1.779e-01 mm.

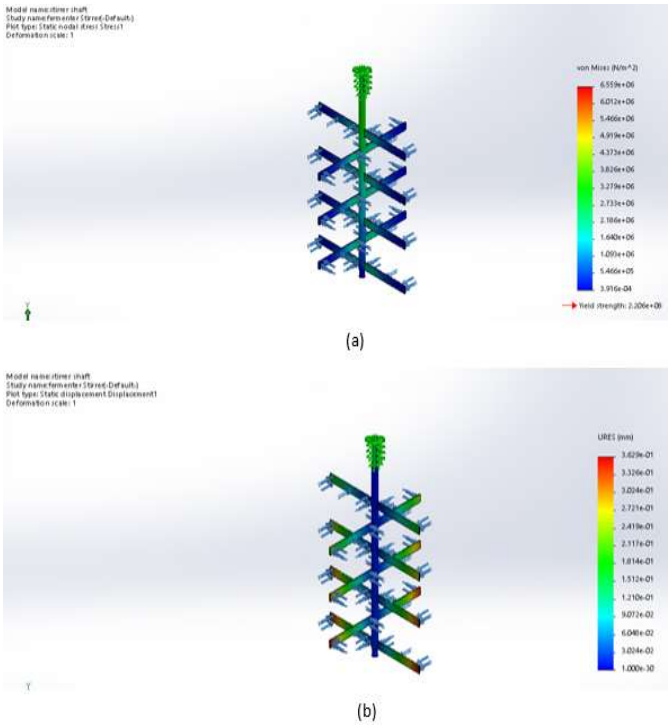

Figure 13 Static (a) stress distributions and (b) displacements of fermenter stirrer

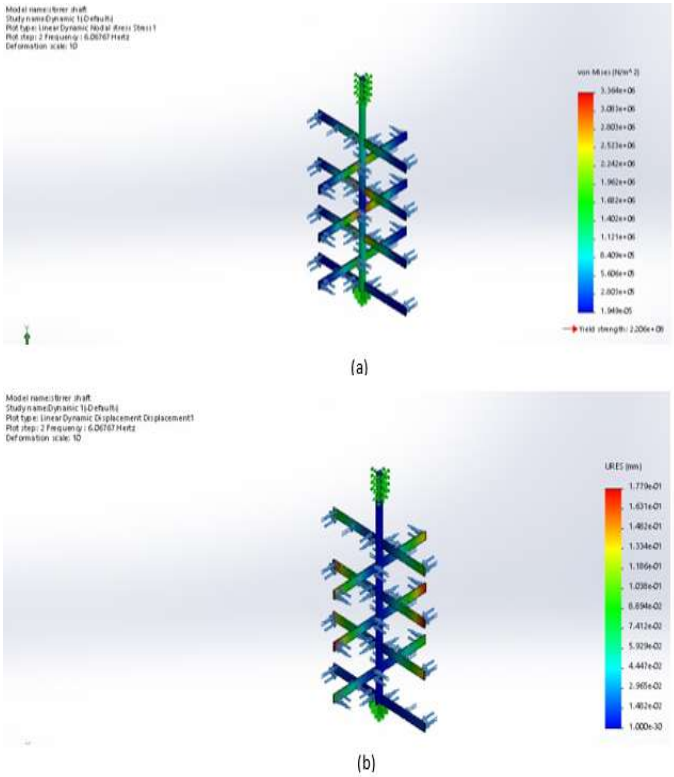

Figure 14 Dynamic (a) stress distribution and (b) displacement of fermenter stirrer

H. Design Evaluation of Auger Shaft

Figure 15 (a & b) present the stress distribution and static displacement of auger shaft. The maximum induced stress was observed to be 6.517e+07 N/m^2 towards both end of the shaft which could be due to load and boundary conditions. Also observed in Figure 15b, is the induced deflection which is at maximum (0.108 mm) at the top of the spiralling blade circling the shaft. However, it was noted that the induced stress was below the yield strength (2.068e+08 N/m^2) of the AISI 304 stainless selected for the design with minimum factor of safety of 3.4 as seen in Table 2. This indicates that the material is unlikely to yield to failure under the design conditions and service requirements (Daniyan *et al.,* 2019).

From the dynamic analysis presented in Figure 16, at a model frequency of 17.76 Hz, the maximum dynamic stress is 5.841e+04 N/m^2 which is far less than the yield strength of the material selected for the shaft. With this, it can be said that the shaft is dynamically safe. This point is also confirmed from the vibration amplitude, where the maximum amplitude is very low at a value of 2.914e-04 mm as seen in Figure 16b.

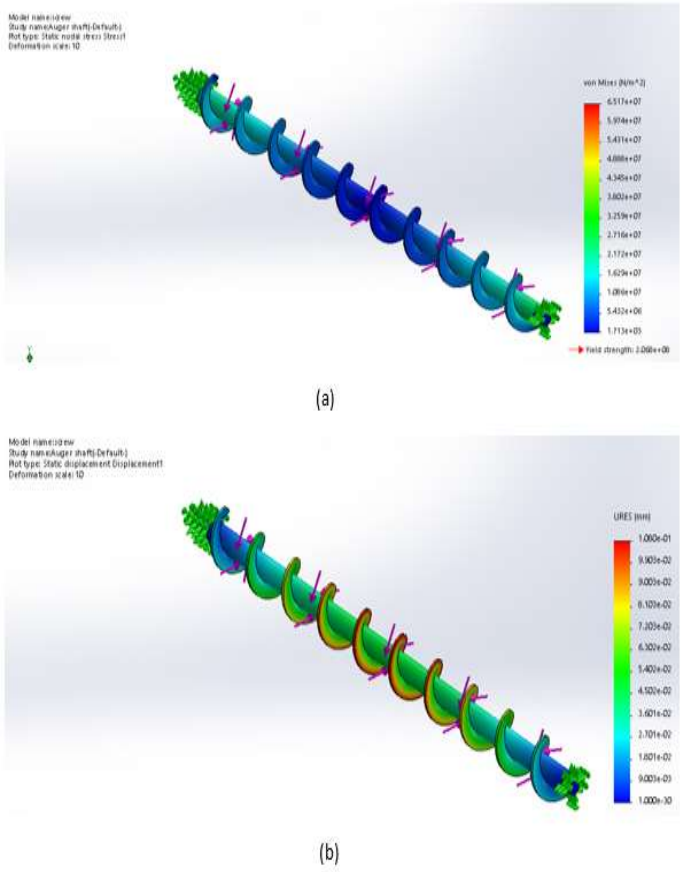

Figure 15 Static (a) stress distributions and (b) displacements of auger shaft

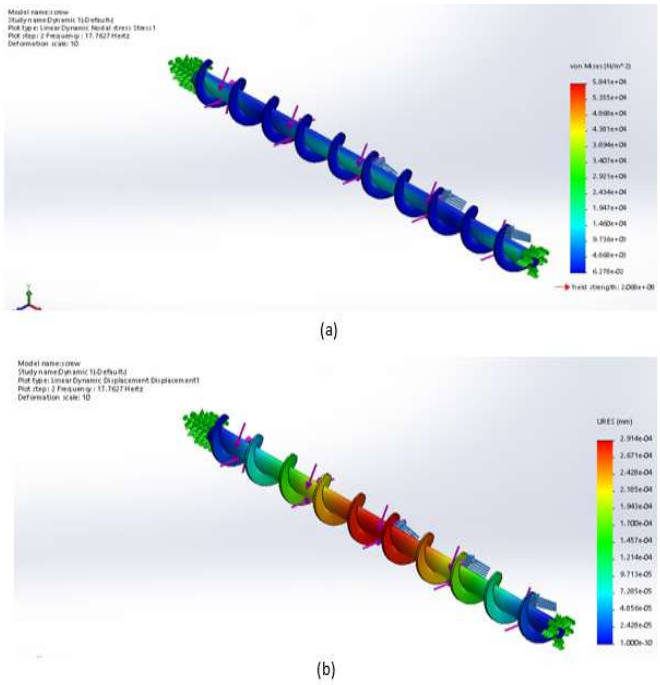

Figure 16: Dynamic (a) stress distribution and (b) displacements of auger shaft

I. Validation of the Simulation Results

The validation results were validated by computing the allowable stresses of the components using American Society of Mechanical Engineers (ASME) conservative allowable stress guideline which specifies that it must be taken as two-thirds of the yield strength (American Society of Mechanical Engineers, 2023). From the FEA simulation, the maximum von Mises stress for the designed stainless steel boiler is 11.62 MPa. The ASME (2023) allowable stress at room or mild service temperature for a typical austenitic stainless steel, is approximately two-thirds of the yield (approximately 160 MPa for the mild steel with 240 MPa yield strength employed for the design, thus, the simulated stress is significantly below the allowable stress. Therefore, the designed boiler component and the proposed material passed the static strength check significantly.

For the designed plain carbon steel de-husking and separation unit, the maximum von Mises stress is 4.954 MPa. The material (plain carbon steel) yield strength is 220.594 MPa, thus, using ASME conservative allowable stress of two-thirds of the yield strength (approximately 147.1 MPa), then the induced stress is significantly than the allowable; therefore the component passes the static strength check significantly. The maximum von Mises stress for the designed mild steel fermenter is 44.87 MPa. For a typical mild steel grade with yield strength of approximately 250 MPa), the conservative allowable which is two-third of the yield strength is approximately 166.7 MPa). Therefore the component passes the static strength check significantly. The allowable stress for the auger shaft and drying unit was found to be approximately 147. 1 MPa while their maximum stressed induced were 65.17 $x10^7$ N/m^2 and 12.67 x 10^7 N/m^2 respectively.

This validation process was done for all the components and it was found that the induced stress was significantly lower than the allowable stress (taken as two-third of the yield strength) in line with the ASME Boiler and Pressure Vessel Code ASME (2023). This implies that the components are designed with the safe limits.

IV. CONCLUSION

The aim of this study was to design and simulate the various components of a locust bean production plant to address the challenges posed by traditional methods of locust bean production, such as poor quality, low production, poor packaging, seed degradation and wastage. This was achieved using computer aided modeling and simulation software (SolidWorks 2016), The simulation results shows that the various stresses induced in the components such as the boiler chamber, boiler frame, de-husking chamber, separating chamber, fermentation chamber, fermenter frame, auger shaft and dryer frame were lower than the yield strength of the materials selected with minimal strain and displacements and factor of safety greater than 1. This implies that the various components will likely meet the service requirements without yielding to failure under the normal working conditions. This study presents empirical data that can be useful for the improving the existing designs locust bean production plants to promote high quality production of locust beans. However, there is still room for improving the performance of the various plant's components through the optimization of the process parameters for the development of various component of the plant with a view to further increase the obtained FOS value. The empirical results presented in this study can assist manufacturing industries to modernize the locust bean production techniques and create a high-quality product that can compete with other food seasonings. This study is limited to design and structural analysis using the finite element analysis technique. Future work can consider the development of the plat using the designed values and optimization of the process parameters.

AUTHOR CONTRIBUTIONS

S. P. Ayodeji: Conceptualization, Data curation, Fund acquisition, Investigation, Methodology, Project Administration, Resources, Software, Validation, Visualization, Writing – original draft. **R. Oboh:** Conceptualization, Data curation, Fund acquisition, Investigation, Methodology, Project Administration, Resources, Software, Supervision, Validation, Visualization, Writing – original draft., Writing – review & editing. **J. T. Isinkaye:** Conceptualization, Fund acquisition, Software, Validation, Methodology Writing – original draft. **I. A. Daniyan:** Conceptualization, Fund acquisition, Software, Validation, Methodology, Writing – original draft

A. O. Adeodu: Fund acquisition, Software, Validation, Methodology**,** Writing – review & editing. **H. S. Phuluwa:** Fund acquisition, Software, Validation, Methodology**,** Writing – review & editing.

REFERENCES

Aborisade, C. A.; L. M. Bakare and F. O. Balogun (2021). Elemental characterization of African locust beans (Parkia biglobosa) in Igbope, Oyo State of Nigeria. Asian Journal of Applied Sciences, 9(2):127-132.

Adekanye, T. A.; E. A. Alhassan; A. A. Okunola; A. D. Iliyah; C. O. Erinle; I. B. Familoni and A. Olaniyi (2019). Evaluation of a locust beans seed dehulling machine for small scale farmers. International Journal of Mechanical Engineering and Technology, 10(3):273–283.

Adewumi, B. A. and A. P. Olalusi (1998). Performance evaluation of a concave type manually operated locust bean dehuller. J. Agric. Technol. 6:22–23.

Ajayi, O. A.; I. M. Akinrinde and O. O. Akinwunmi (2015). Towards the development of shelf stable "iru" (Parkia Biglobosa) condiment bouillon cubes using corn, cassava and potato starch extracts as binders. Niger. Food. J. 33:67–72.

Akande, F. B.; O. A. Adejumo; C. A. Adamade and D. Bodunde (2010). Processing of locust bean fruits: challenges and prospects. African Journal of Agricultural Research, 5(17): 2268-2271

Alabi, D. A.; O. R. Akinsuhre and M. A. Sanyaolu (2005). Quantitative determination of chemical and nutritional composition of Parkia biglobosa (Jacq) Berth. African Journal of Biotechnology, 4(8): 4-6.

American Society of Mechanical Engineers (2023). ASME Boiler and Pressure Vessel Code: Section VIII—Rules for Construction of Pressure Vessels, Division 1. ASME. Available at https://dl.gasplus.ir/standard-ha/Standard-ASME/ASME%20BPVC%202023%20Section%20VIII%20div.%201.pdf [accessed 18th October, 2025].

Audu, I.; A. Oloso and B. Umar (2004). Development of a concentric cylinder locust bean dehuller. Agricultural Engineering International: The CIGR Journal of Scientific Research and Development, 04003.1(11)

Ayodeji, S. P.; M. K. Adeyeri and O. Olabanji (2012). Design of a process plant for the production of poundo yam. International Journal for Engineering Modelling, 6(1): 10-24

Beaumont, M. (2002). Flavouring composition prepared by fermentation with Bacillus spp. International Journal Food Microbiology, 75:189-196

Budynas, R. G. and K. J. Nisbett (2011). Shigley's Mechanical Engineering Design. 9th Edition (McGraw-Hill Series in Mechanical Engineering).

Daniyan, I. A.; A. O. Adeodu; B. I. Oladapo; O. L. Daniyan and O. R. Ajetomobi (2019). Development of a reconfigurable fixture for low weight machining operations. Cogent Engineering, 6: 1579455, pp. 1-17.

Daniyan, I.; F. Ale; F. Fameso; S. Mrausi and J. Ndambuki (2024). Computer aided simulation and experimental investigation of the machinability of Al 6065 T6 during milling operation. International Journal of Advanced Manufacturing Technology, 133(1-2):589–607.

Diawara, B.; L. Sawadogo; W. F. Amoa-Awua and M. Jakobsen (2000). Capability building for research and development in quality assurance and fermentation technology for African fermented foods. HACCP system for traditional African fermented foods: soumbala. WAITRO Journal, 26: 11-62.

Engineering ToolBox (2001). [Online] Available at: https://www.engineeringtoolbox.com [Accessed 05-01-2023].

Fameso, F. and D. Desai (2020b). Explicit analysis using time-dependent damping simulation of one-sided laser shock peening on martensitic steel turbine blades. Simulation, 96(12):927-938.

Fameso, F.; D. Desai; S. Kok; D. Armfield and M. Newby (2022). Residual stress enhancement by laser shock treatment in chromium-alloyed steam turbine blades. Materials, 15(16):5682.

Fameso, F.; D. Desai; S. Kok; M. Newby and D. Glaser (2020a). Simulation of laser shock peening on x12cr steel using an alternate computational mechanical threshold stress plasticity model. The International Journal of Advanced Manufacturing Technology, 111:1-11.

Farayola, C. O.; V. Okodu and O. O. Oni (2012). Economic analysis of locust beans processing and marketing in Ilorin, Kwara State. International Journal of Agricultural Research, Innovation and Technology, 2(2): 36-43

Gbabo, A.; J. T. Liberty and O. S. Fadele (2013). Design, Construction and Assessment of African Locust Bean (Parkia Biglobosa) Dehuller and Separator. Int. J. Eng. Innovat. Technol. 3:438–444.

Gberinko, G. M.; J. B. Ameh; S. A. Ado and V. J. Umoh (2014). Physicochemical properties of powdered condiments of Parkia Biglobosa fermented with and without mixed bacillus species A and B as Inocula and subjected under different drying conditions. Arch. Appl. Sci. Res. 6, 115–120.

Helmenstine, T. (2021). Calculate energy required to turn ice into steam. [Online] Available at: https://www.thoughtco.com/ice-to-steam-energy-calculation-609497 [Accessed 05-01-2023]

Khurmi, K. S. and J. K. Gupta (2005). Machine Design. 14th ed.; S. Chand and Company Ltd., RAM Nagar, New Delhi, India. 434 – 960.

Kourouma, K.; C. G. Jean; E. A. Achille and A. Clement (2011). Ethnic differences in use values and use patterns of Parkia biglobosa in Northern Benin. Journal of Ethnobiology and Ethnomedicine, 7(1): 42

Koya, O. A.; B. S. Ogunsina and O. O. Opeyemi (2011). Deformation and Dehulling of Sponge Gourd (Luffa aegyptiaca) Seeds. International Journal of Food Properties, 14(2): 432-440

Muvunzi, R.; K. Mpofu; I. A. Daniyan and F. Fameso (2022). Analysis of potential materials for local production of a rail car component using additive manufacturing. Heliyon, 8(e09405):1-8.

Ogunjimi, L. A.; N. A. Aviara and A. Omotayo (2002). Some engineering properties of locust seed. Journal of Food Engineering. 55(2): 95-99.

Okunola, A. A.; T. A. Adekanye; A. Ayooluwa; C. B. Okonkwo; S. A. Alake; T. M. A. Olayanju and A. D. Adewumi (2019). Development of a locust bean seed dehulling cum washing machine. International Journal of Mechanical Engineering and Technology, 10(1): 1321-1330

Olajide, R. (2012). Growth performance, carcass, haematology and serum metabolites of broilers as affected by contents of anti-nutritional factors in soaked wild cocoyam (Colocasia esculenta (L.) Schott) corm-based diets. Asian J. Anim. Sci., 6: 23-32.

Owolarafe, O. K.; D. A. Adetan; G. A. Olatunde; A. O. Ajayi and I. K. Okoh (2013). Development of a locust bean processing device. J. Food Sci. Technol. 50, 248–256.

Oyesola, M. O.; K. Mpofu; I. A. Daniyan and N. Mathe (2022). Design and simulation of a bearing housing aerospace component from titanium alloy (Ti6Al4V) for additive manufacturing. Acta Polytechnica 62(6):639–653.

Rogers, G. F. and Y. R. Mayhew (1995). Thermodynamic and Transport Properties of Fluids SI Units. Fifth Edition. Blackwell Publishing.

Sadiku, O. A. (2010). Processing Methods Influence the Quality of Fermented African Locust Bean (Iru/ogiri/dadawa) Parkia biglobosa. Journal of Applied Sciences Research, 6(11): 1656-1661

Uzodinma, E. O.; C. F. Okoyeuzu; N. N. Uchegbu; C. O. Okpala; W. A. Rasaq; I. Shorstkii; G. Sardo; G. Bono and M. Korzeniowska (2021). Cubing fabrication/costing and machine performance on African fermented condiment quality attributes compared with commercial bouillon types. Processes, 9(3), 481.

Uzodinma, E. O.; C. F. Okoyeuzu; N. N. Uchegbu; C. O. R. Okpala; W. A. Rasaq; I. Shorstkii; G. Sardo; G. Bono and M. Korzeniowska (2021). Cubing Fabrication/Costing and machine performance on African fermented condiment quality attributes compared with commercial bouillon types. Processes 2021, 9, 481.